

# Structural Evolution, Dielectric Studies and Energy Storage Performance of Barium Calcium Zirconium Titanate Ceramic Synthesized by Solid State Reaction Method

Pawan Kumar, Anjali Oudhia

Dept. of Physics, Govt. Nagarjuna PG College of Science, Raipur, Chhattisgarh, 492001, India

G Nag Bhargavi

Dept. of Physics, Govt. Pt. Shyamacharan Shukla College Dharsiwa, Raipur Chhattisgarh. 493221, India

Tanmaya Badapanda,

Dept. of Physics, C V Raman Global University Bhubaneswar, Odisha 751029, India

Sanjib Kumar Rout

Dept. of Physics, Birla Institute of Technology, Mesra, Ranchi, Jharkhand 835215, India

## Abstract

In the present day the increasing demand of environmental protection and human health concerns are motivating the researchers to develop lead-free ceramics for various applications. Barium Calcium Zirconium Titanate (BCZT) is a lead-free ceramic which is recently studied for energy storage applications. The present work demonstrates the structural, micro structural and electrical behavior of BCZT perovskite ceramic. The BCZT ceramic with chemical composition  $\text{Ba}_{0.85}\text{Ca}_{0.15}\text{Zr}_{0.1}\text{Ti}_{0.9}\text{O}_3$  is prepared by the high temperature solid state diffusion method. A phase pure polycrystalline compound is obtained after calcination at  $1300^\circ\text{C}$ . The phase formation is confirmed by X ray diffraction (XRD) and Raman spectroscopic studies which confirm the tetragonal phase of the crystals. Scanning electron microscopy (SEM) image indicates the formation of well- developed grains having grain size of  $3.3\ \mu\text{m}$ . The electrical behavior of the prepared sample is studied and discussed in terms of dielectric and ferroelectric properties. The dielectric study of BCZT showed normal phase transition behavior from ferroelectric to paraelectric phase at  $83^\circ\text{C}$ . The diffusivity analysis was used for better comprehension of the electrical processes in the materials. The ferroelectric hysteresis loops were obtained at different temperatures and voltages. The energy storage efficiency of the ceramic was increasing with temperature and the maximum efficiency was 44.3% at  $125^\circ\text{C}$  for an electric field of  $15\text{kV/cm}$ .

**Keywords:** Solid state reaction method; XRD; SEM; Dielectric studies; Ferroelectric studies

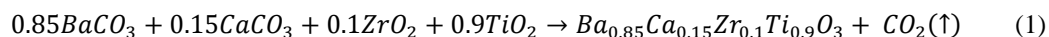
## 1. INTRODUCTION

The development of lead-free piezoelectric ceramics has drawn great attention these days due to growing environmental concerns. Study of ferroelectric materials is of significant importance for various useful applications such as Multilayer ceramic capacitors, dynamic random-access memories, transducers, optical waveguides, micro-sensors and actuators etc. [1–5]. Oxide perovskites with general formula  $\text{ABO}_3$  are best known ceramic materials for these applications. In  $\text{ABO}_3$  structure, A and B both are cations of different ionic radius and charge states and O is oxygen.  $\text{BaTiO}_3$  (BT) is a commonly known perovskite with Ba atoms as A-site cations and Ti atoms as B-site cations. A complex perovskite system like  $A'_x A''_{(1-x)} B'_y B''_{(1-y)} \text{O}_3$  can be obtained by the substitution of suitable cations both at A and B sites. The solid solution of Barium Zirconate ( $\text{BaZrO}_3$ )- Barium titanate ( $\text{BaTiO}_3$ ) known as Barium Zirconate Titanate ( $\text{BaZrTiO}_3$ ) represents a promising class of dielectric materials [6-8]. The phase diagram of Barium Zirconate

Titanate (BZT) shows a cubic structure above the Curie temperature [9, 10]. Below the Curie temperature it crystallizes to tetragonal phase or rhombohedral phase depending upon the Zr/Ti ratio in the BZT system. The region between these rhombohedral and tetragonal phases of the sample is called the morphotropic phase boundary (MPB). In this region, the material has high dielectric, ferroelectric and piezoelectric properties [11-14]. In attempts to improve the physical properties of BZT, dopants are generally added to the Ba or Zr or Ti sites of the material.  $\text{Ca}^{2+}$  doped  $\text{BaTiO}_3$  ceramics known as Barium Calcium Titanate (BCT) have been used to make multilayer capacitors, memory devices, electro-optic modulators, dielectric antennas, multiplexers, resonators, and dye decolorization through piezocatalytic and photocatalytic activities [15-18]. The BCT composition possesses three incongruities related to rhombohedral (R), tetragonal (T), orthorhombic (O), and cubic (C) transitions, and the phase transition temperature from rhombohedral to orthorhombic decreases remarkably with doping concentration. Similarly, the BZT system possesses compositional dependence for the improved dielectric and ferroelectric properties. For the Zr/Ti ratio less than 15/85 normal dielectric behaviour is seen whereas for the compositions with higher percentage of Zr possesses relaxor behaviour. The BZT system with Zr/Ti ratio in between 10/90 to 20/80 possesses one dielectric irregularity related to R-C above the room temperature with a very less frequency dispersion effect. To date, considerable research efforts have been devoted to improving the dielectric and ferroelectric properties of BT based ceramics. Studies have been carried out for co-doping of Ca and Zr in the BT resulting in a solid solution with the general formula  $\text{Ba}_{1-x}\text{Ca}_x\text{Ti}_{1-y}\text{Zr}_y\text{O}_3$  (BCZT) [18-23]. The morphotropic phase boundaries found in the BCZT system have improved the dielectric, ferroelectric and piezoelectric properties which are evident in the earlier work. It is found from the literature that the composition  $\text{Ba}_{0.85}\text{Ca}_{0.15}\text{Ti}_{0.9}\text{Zr}_{0.1}\text{O}_3$  (BCZT) is one of the potential candidates as lead-free piezoelectric ceramics which have a high piezoelectric coefficient and high planar electromechanical coefficient [24]. Orlik et al. found that the  $\text{Ba}_{0.85}\text{Ca}_{0.15}\text{Ti}_{0.90}\text{Zr}_{0.10}\text{O}_3$  ceramic with a phase coexistence structure exhibits a giant piezoelectricity ( $d_{33} = 330 \text{ pC/N}$ ) [25]. Wu et al. obtained excellent piezoelectric properties ( $d_{33}=540 \text{ pC/N}$ ,  $k_p=0.42$ ) in  $\text{BaZr}_{0.2}\text{Ti}_{0.8}\text{O}_3-0.2\text{Ba}_{0.7}\text{Ca}_{0.3}\text{TiO}_3-0.3\text{Ba}_{0.7}\text{Sr}_{0.3}\text{TiO}_3$  leadfree material by constructing R-T phase boundary [26, 27]. Among this family,  $x[\text{Ba}(\text{Zr}_{0.2}\text{Ti}_{0.8})\text{O}_3]-(1-x)[(\text{Ba}_{0.7}\text{Ca}_{0.3})\text{TiO}_3]$  (BZT-xBCT, BCZT) system has been reported by Liu and Ren [26, 28] to exhibit interesting dielectric, ferroelectric, and piezoelectric properties at the morphotropic phase boundary (MPB) which is comparable to those of PZT ceramics. The high piezoelectric properties of this system are due to the coexistence of two ferroelectric phases at the MPB [29].

## 2. EXPERIMENTAL

$\text{Ba}_{0.85}\text{Ca}_{0.15}\text{Zr}_{0.1}\text{Ti}_{0.9}\text{O}_3$  ceramic was prepared by the conventional solid-state reaction route. The starting materials as  $\text{BaCO}_3$  (99.8%),  $\text{CaCO}_3$  (99.5%),  $\text{ZrO}_2$  (99.5%) and  $\text{TiO}_2$  (99.8%) (all Merck) were weighed in stoichiometric proportion.  $\text{BaCO}_3$  and  $\text{CaCO}_3$  were provided by S.D. Fine Chem., Mumbai,  $\text{TiO}_2$  and  $\text{ZrO}_2$  were provided by E. Merck India Ltd. and Loba Chem., Mumbai, respectively. The stoichiometric quantities were wet mixed in acetone and distilled water and dried with agate mortar. The homogeneous mixture was calcined in air at  $1300^\circ\text{C}$  for 5 hours in a high temperature furnace. After calcination the structural properties were studied by X-ray diffraction and Raman spectroscopy. For the electrical property measurements, the calcined powder was compacted in the form of discs with 1.0 cm in diameter by uniaxial pressing at 200 MPa with 5 wt% PVA (Polyvinyl Alcohol) solution added as a binder. The discs were then sintered at  $1350^\circ\text{C}$  for 5 hours. Silver electrodes were applied to the opposite disc faces and heated at  $700^\circ\text{C}$  for 5 min. The reaction taking place between the different reagents can be expressed by the following relation:



The synthesized powder was characterized with respect to phase identification and lattice parameter measurements, using  $\text{Cu-K}\alpha$  ( $\lambda=1.541 \text{ \AA}$ ) X-ray diffraction (XRD) with the help of Pananalytical X'pert Pro Diffractometer. The lattice parameters were calculated using X'pert Highscore software. The surface morphology was observed and the average grain size was measured through scanning electron microscope (Zeiss Make EVO 18 scanning electron microscope). For Raman spectroscopic studies, Jobin Yvon Horiba, France make spectrometer (model T64000) with argon–krypton mixed ion gas laser (Spectra Physics Make, USA, model 2018 RM) was used. An LCR Meter (N4L-NumetriQ LCR meter, model PSM1735) was used to measure the dielectric properties of silver pasted BCZT pellets in the frequency range of 1 Hz to 1 MHz. The ferroelectric hysteresis loops were determined by using a ferroelectric test system (Marine India make P–E loop tracer).

### 3. RESULTS AND DISCUSSION

#### 3.1 Structural Study

The phase formation of the BCZT ceramic and its structure was verified through X-ray diffraction characterization technique. Fig. 1 displays the XRD data obtained in the angular range of  $10^\circ < 2\theta < 80^\circ$ . The XRD pattern of BCZT ceramic at room temperature exhibits pure perovskite phase which is calcined at  $1300^\circ\text{C}$  for 5 hours. The XRD peaks obtained are analyzed using X'pert high score plus software. The sharp intense and well-defined diffraction peaks indicate that the ceramic material has a tetragonal phase with "P4mm" space group as confirmed by JCPDS No. 79-2265. The presence of any deleterious phase is not witnessed that confirms the formation of single-phase compound with long range crystallinity. The highest intensity peak is observed at  $31.9^\circ$  which is indexed as (110). The obtained peaks are further analyzed using "Checkcell" software to determine the cell parameters. All the reflection peaks of the X-ray profile are indexed and lattice parameters are determined using a least-squares method with the help of "Checkcell". Good agreement between the observed and calculated interplanar spacings ( $d$ -values) is seen. The observed and calculated  $d$ -values are listed in Table 1. The calculated values of cell parameters are;  $a=b=4.0023\text{ \AA}$ ,  $c=4.0092\text{ \AA}$ ;  $\alpha=\beta=\gamma=90^\circ$ ; and cell volume  $V=64.22\text{ \AA}^3$ . In Perovskite compounds, the tetragonality is measured in terms of  $c/a$  ratio. The tetragonality in the samples can also be measured in terms of tolerance factor ( $t$ ). In the perovskite structure, the tolerance factor is often used to determine the structural stability, which can be calculated from Eq.

$$t = \frac{R_O + R_A}{\sqrt{2(R_O + R_B)}} \quad (2)$$

Where  $R_A$ ,  $R_B$  and  $R_O$  are the ionic radii of A-cation, B-cation and Oxygen ion. For an ideal perovskite structure with cubic symmetry, the value of ' $t$ ' is unity. However, stable perovskite structures with noncubic symmetry can be obtained when ' $t$ ' deviates from unity. The tolerance factor of a complex system like  $AB'_xB''_{(1-x)}O_3$  is given by the Eq.

$$t = \frac{R_O + R_A}{\sqrt{2(R_O + xR_{B'} + (1-x)R_{B''})}} \quad (3)$$

The tolerance factor of  $\text{Ba}_{0.85}\text{Ca}_{0.15}\text{Zr}_{0.1}\text{Ti}_{0.9}\text{O}_3$  perovskites is theoretically calculated using the following formula:

$$t = \frac{R_O + 0.85R_{\text{Ba}^{2+}} + 0.15R_{\text{Ca}^{2+}}}{\sqrt{2(R_O + 0.1R_{\text{Zr}^{4+}} + 0.9R_{\text{Ti}^{4+}})}} \quad (4)$$

where,  $R_O$ ,  $R_{\text{Ba}^{2+}}$ ,  $R_{\text{Ca}^{2+}}$ ,  $R_{\text{Zr}^{4+}}$  and  $R_{\text{Ti}^{4+}}$  are the ionic radii of O, Ba, Ca, Zr and Ti ions and the corresponding values are  $R_O=1.40\text{ \AA}$ ,  $R_{\text{Ba}^{2+}}=1.60\text{ \AA}$ ,  $R_{\text{Ca}^{2+}}=0.9\text{ \AA}$ ,  $R_{\text{Zr}^{4+}}=0.72\text{ \AA}$  and  $R_{\text{Ti}^{4+}}=0.6\text{ \AA}$ . The calculated value of ' $t$ ' for BCZT is 1.02 (using relation (4)) it confirms the nonsymmetric perovskite structure in the sample. Since the ionic radii of Zr and Ti are different, a distortion in  $\text{ZrO}_6/\text{TiO}_6$  octahedra takes place. As a result of which a disorderness as well as lattice strain develops in the ceramic.

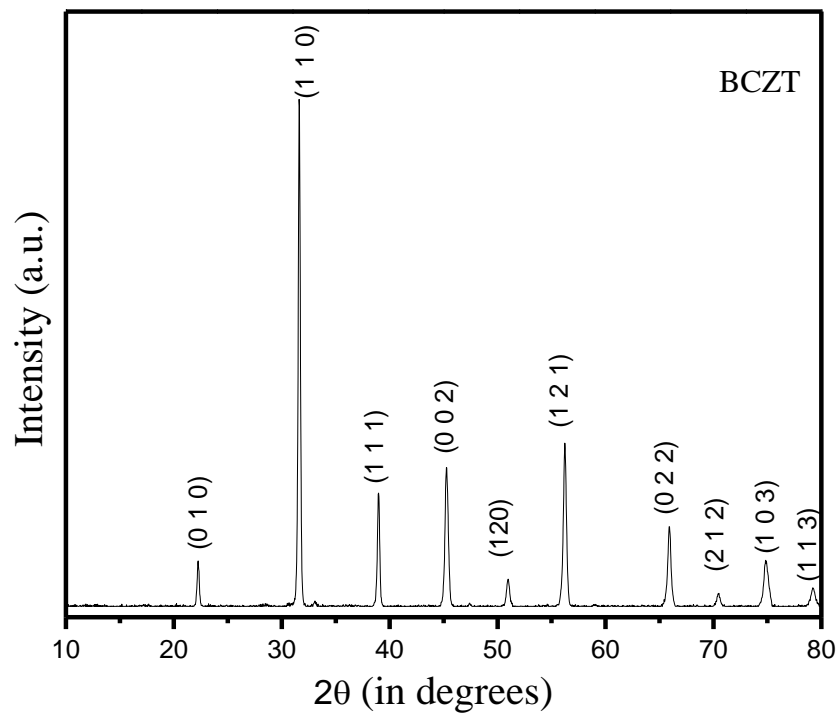


Fig. 1 X-ray diffraction patterns of BCZT ceramic calcined at 1300 °C

The surface and grain morphology of the prepared sample is studied by SEM. The SEM micrograph of the microcrystalline BCZT ceramic pellet sintered at 1350°C is shown in the fig. 2 which is characterized by well-developed grains with irregular shape. Here we observed that the grains are well developed along with sharp edges and well-defined borders. The surface of the sample displays a tight and condensed morphology with very less pores and distinct grain boundaries and seldom pores. We observed uniformity in the grains are their size is in the order of few microns. The SEM also shows lamellar structures in BCZT (indicated with blue frame circle). A representative histogram of the grain size distribution of BCZT is shown in Fig. 2(b). The average grain size of the sample is about 10µm.

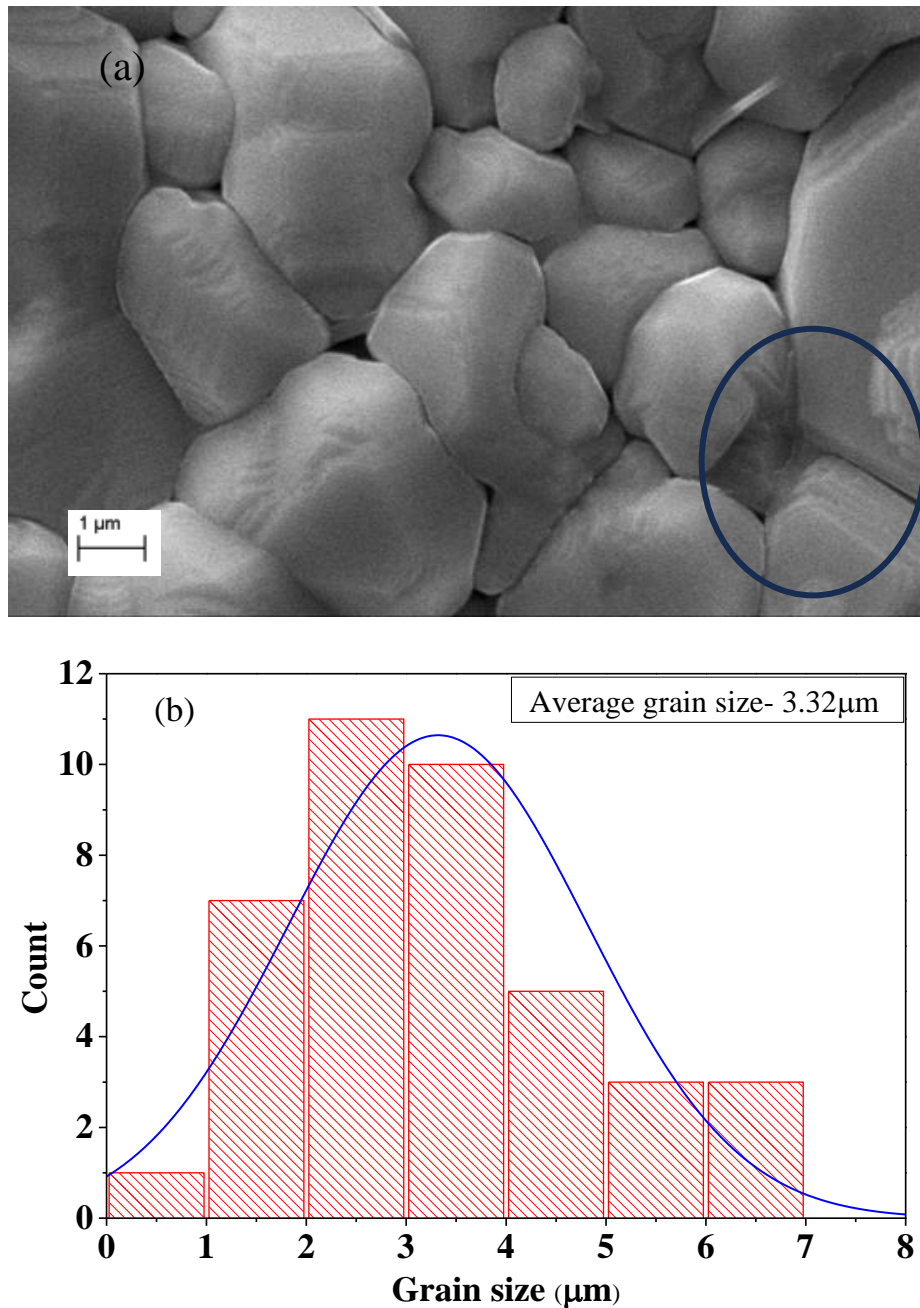


Fig. 2(a) SEM micrograph of BCZT ceramic pellet sintered at 1350°C (b) grain size distribution of BCZT pellet

Raman spectroscopy is a non-destructive method used to identify the phase transitions of complex ferroelectric materials. Fig. 3 presents the Raman spectra of BCZT ceramic where the Raman bands (position and intensity) are noticed in the range of 200-800  $\text{cm}^{-1}$ . Here we witnessed two Raman active modes of BCZT as shown in the figure. Raman peaks are observed around 477  $\text{cm}^{-1}$  and 697  $\text{cm}^{-1}$ . These are characteristic to the ferroelectric phases (rhombohedral, orthorhombic and tetragonal) of BCZT ceramic. Ba-O bonds produce two mixed modes, [A1/E(TO)] and [A1/E(LO)]. These results suggest the presence of tetragonal distortion in the BCZT ceramic. Also, these modes are broad which indicates the polycrystalline nature of the sample.

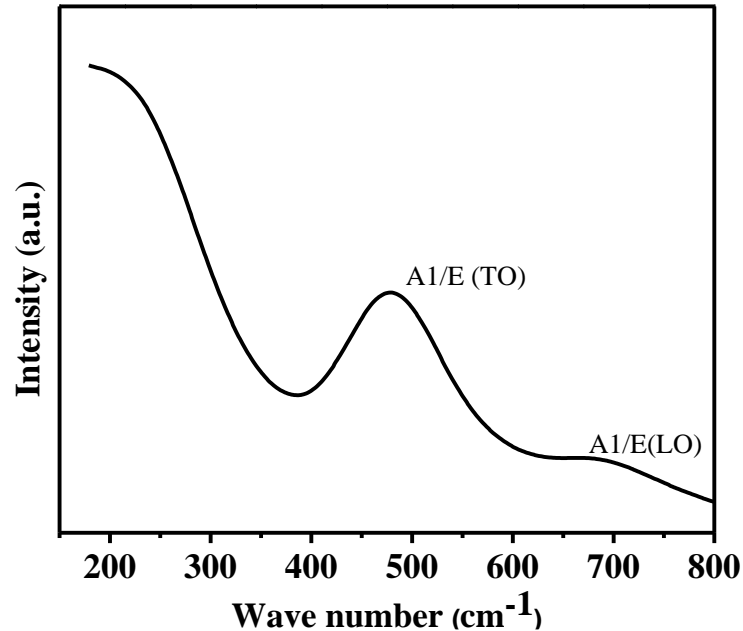


Fig. 3 Raman spectra of BCZT ceramic at room temperature

### 3.2 Dielectric studies

The dielectric constant of the ceramic is measured using the eq. given below:

$$\epsilon_r = \frac{Cd}{\epsilon_0 A} \quad (5)$$

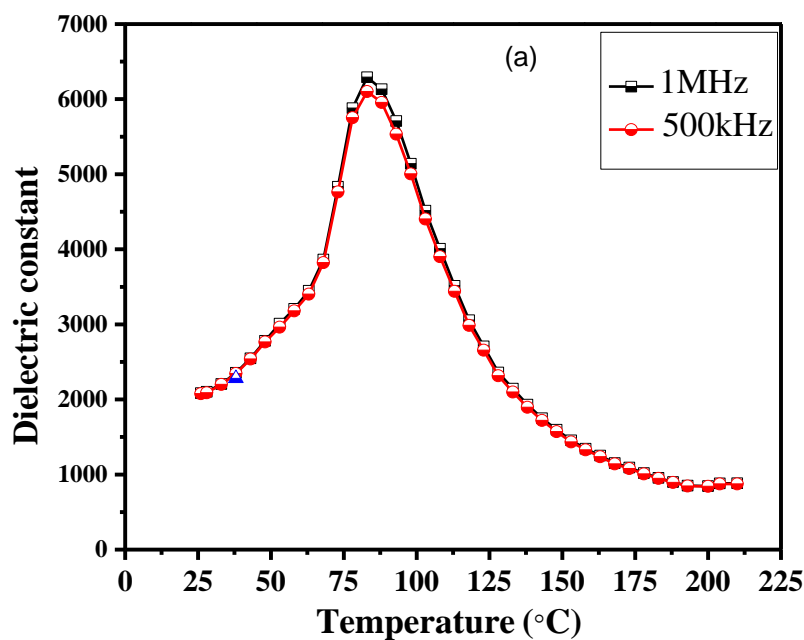
Where, C is the capacitance (F) of the ceramic,  $\epsilon_0$  is the permittivity of the free space ( $8.855 \times 10^{-12}$  F/m), A is the electrode area ( $m^2$ ) of the ceramic pellet, and d is the thickness (m) of the ceramic pellet made in the form of capacitor. The relative permittivity (dielectric constant) of BCZT ceramic as a function of temperature at frequencies 500kHz and 1MHz is displayed in fig. 4(a). The dielectric constant of BCZT ceramic has shown a traditional behaviour with temperature. For both the frequencies, dielectric constant at first increases to its maximum value ( $\epsilon_m$ ) and then decreases smoothly. This represents a structural phase transition in BCZT ceramic. The graph depicts structural phase transitions at 83°C ( $T_c$ ). The sharp peak at 83°C (Curie temperature) represents the transition temperature ( $T_c$ ), which is associated to polarized ferroelectric phase (tetragonal) to unpolarized paraelectric (cubic) phase transition. It has been claimed that the crystal structure and grain size had a significant impact on the solid solutions' dielectric characteristics [30-32]. In the entire process of dielectric measurement, the permanent dipole moment is affected by polarization. It is again noteworthy that  $\epsilon_r$  value is significantly influenced by the dopant type, dopant ratio, and sintering temperatures. Additionally, there are other both intrinsic and external elements that can be affecting, including grain size, grain boundaries, density, pressure, and domain wall motion. In BCZT the  $Ca^{2+}$  ions at A-site and  $Zr^{4+}$  ions at B-site both influence the dielectric permittivity. The  $Ca^{2+}$  ions have smaller ionic radius and smaller electronic polarizability than  $Ba^{2+}$  ions and hence the  $T_c$  is expected to reduce as compared to the  $T_c$  of  $BaTiO_3$  which is  $\sim 137^\circ C$  [33]. However, the earlier reports mention that there is no significant change in the  $T_c$  with the substitution of Ca, this indicates  $Ca^{2+}$  ions have complex impact on the ferroelectric properties [34, 35]. On the other hand, when  $Ti^{4+}$  ions are replaced by  $Zr^{4+}$  ions producing  $BaZr_yTi_{1-y}O_3$  ceramic, a shift from normal ferroelectric to relaxor ferroelectric behaviour is seen for  $y > 0.2$ . Also, a significant reduction in the  $T_c$  with good dielectric tunability is also observed [6]. For low concentration of Ca the BCZT ceramic show excellent ferroelectric properties because of the off-centered  $Ca^{2+}$  ions and hence the temperature of maximal permittivity shows an increasing trend. However, in the present composition of BCZT ( $Ba_{0.85}Ca_{0.15}Zr_{0.1}Ti_{0.9}O_3$ ) a  $CaTiO_3$  phase occurs and  $Ti^{4+}$  ions being replaced by  $Zr^{4+}$  ions decrease the temperature of maximal permittivity. Additionally, the negatively charged  $O^{2-}$  ions and the positively

charged  $\text{Ti}^{4+}$  ions are slightly displaced from their symmetrical positions which result in upward displacement. So, the distortion along c-axis results in tetragonal phase in the crystal at room temperature. The dielectric behaviour of the sample is in agreement with our XRD data. The dielectric constant has significantly decreased with temperature above  $T_c$ . It means the tetragonal phase (non-centrosymmetric) at low temperature has been transformed into cubic (centrosymmetric) phase at high temperature. Thus, above  $T_c$  the crystalline phase is paraelectric which has no permanent dipole moment. The dielectric loss ( $\tan\delta$ ) of BCZT ceramic as a function of temperature at frequencies 500kHz and 1MHz is shown in fig. 4(b). The results show that the dielectric loss change a little in the temperature range of 30–200 °C. The  $\tan\delta$  curves have slight fluctuations and confirm that the dielectric loss is less than 0.1 in the wide temperature range which indicates that  $\tan\delta$  is not sensitive to temperature. The variation of dielectric constant with frequency is shown in fig. 5 which shows a normal trend i.e. higher at low frequencies and keep on decreasing with increasing frequencies.

In order to describe the dielectric relaxation behavior of ceramics, several models have been proposed, among which the popular one is the modified Curie–Weiss law given as:

$$\frac{1}{\epsilon'} - \frac{1}{\epsilon'_{max}} = \frac{(T-T_m)^\gamma}{C} \quad (6)$$

where  $\epsilon'_{max}$ ,  $C$  and  $\gamma$  are the dielectric permittivity at  $T_m$  (the dielectric-temperature curve reaches maxima at  $T_m$ ), the Curie-like constant, and the degree of dielectric relaxation ( $1 \leq \gamma \leq 2$ ), respectively.  $\gamma=1$  corresponds to a normal ferroelectric while,  $\gamma=2$  is labeled as perfect relaxor. In this study the diffusivity in the sample is obtained by plotting a graph between  $\log(1/\epsilon' - 1/\epsilon'_{max})$  and  $\log(T-T_m)$  for 500 kHz frequency, presented in fig. 6. The graph follows Curie-Weiss law showing a linear relationship between plotted quantities. In this study, the value of diffuseness coefficient ( $\gamma$ ) is found to be 1.7, which indicates the dielectric properties are tending towards diffuse ferroelectric behavior. The broadness or diffuseness occurs mainly due to compositional fluctuation and structural disordering in the arrangement of cation at one or more crystallographic sites of the structure.



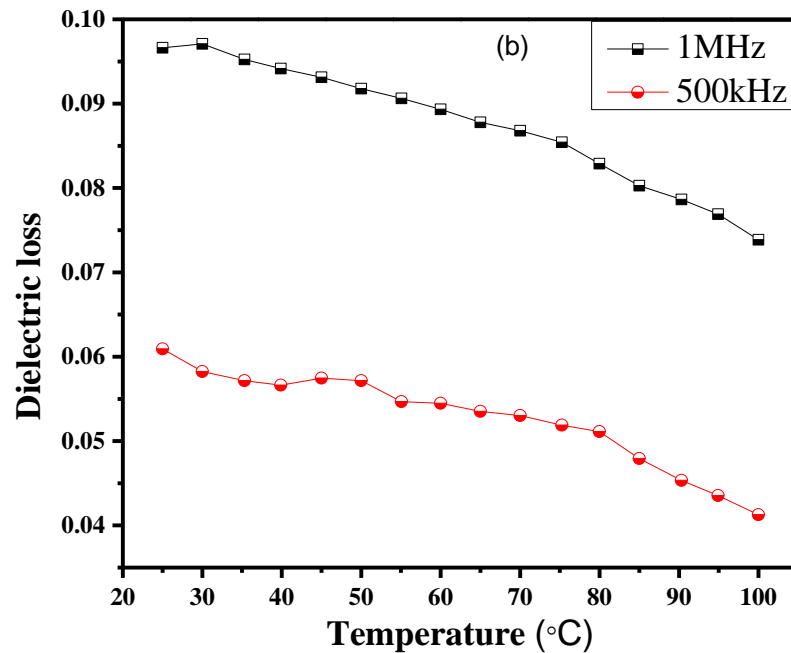


Fig 4(a) Dielectric constant and (b) dielectric loss of BCZT ceramic as a function of temperature at 500kHz and 1MHz

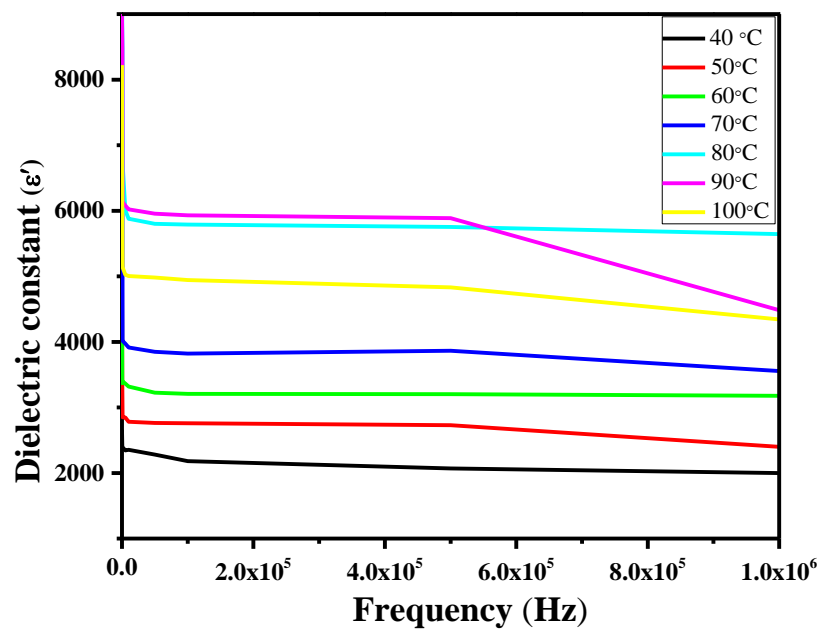


Fig. 5 Dielectric constant of BCZT ceramic as a function of frequency at different temperatures

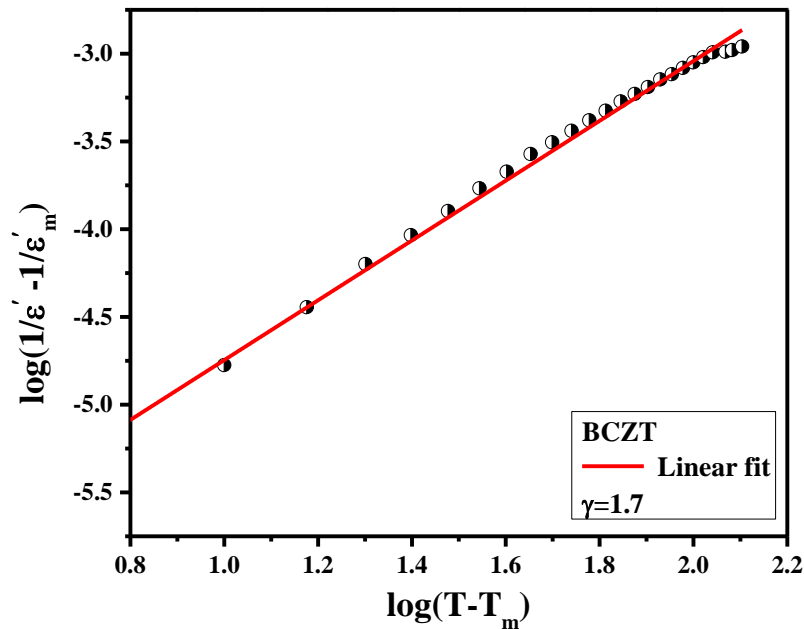


Fig. 6 Dielectric permittivity data fitted to the modified Curie–Weiss law for BCZT ceramic at 500 kHz

### 3.3 Ferroelectric studies

The ferroelectric properties (PE loops) of a ceramic are important for investigation of phase evolution. In BCZT ceramic the off-centering of  $\text{Ti}^{4+}/\text{Zr}^{4+}$  ions within the  $\text{TiO}_6/\text{ZrO}_6$  octahedra are responsible for the ferroelectric properties. The PE loops of BCZT ceramics are shown in fig. 7 where the effect of temperature can be seen. The hysteresis loops between polarization (P) and electric field (E) are exhibited (fig. 7) with increasing temperatures from 25°C to 125°C at an electric field of 15kV/cm. The sample exhibit a well visible hysteresis loop. All the ceramics have a typical characteristic i.e. the ferroelectric properties increase with increasing temperature also representing the ferroelectric to paraelectric phase transition. It is observed that the PE loops are slimmer at higher temperatures gradually tending towards linearity but do not completely become linear even after phase transition temperature (83 °C) indicating hysteresis loss in the sample. From the PE loops analysis some diffuseness in phase transition behavior of BCZT sample is seen where the similar behaviour is observed in dielectric vs. temperature studies too.

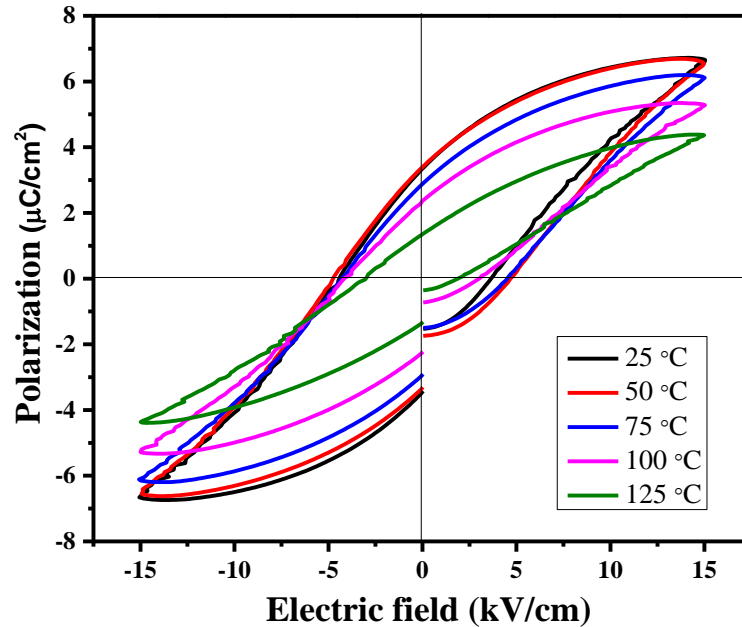


Fig. 7 P-E loops of BCZT ceramics at different temperatures sintered at 1350°C

Fig. 8 shows the variation of remnant polarization ( $P_r$ ) and coercive field ( $E_c$ ) with temperature. Remnant polarization and coercive field both found to decrease when the temperature is increasing. The thermal fluctuations significantly effect the ferroelectric interaction between the dipoles and also the lattice distortion. As a result of which the  $P_r$  values decrease. However, the reduction in  $E_c$  indicates the softening of sample on heating [36]. As per the earlier discussion the area under the hysteresis loops is decreasing when the temperature is increasing, this is certainly because the area under the loop is directly proportional to the domain wall motion. At low temperatures the domain wall motion is slow and hence the area under the loops is large further with increasing temperature the domain wall motion becomes fast and hence the loop area decreases. Even some polarization is still witnessed beyond the transition temperature. The remnant polarization is largely influenced by the grain size. Larger the grain size better is the ferroelectric property. The SEM results of BCZT ceramic confirms the larger grain size which is in agreement to better ferroelectric properties. Further, the decreasing coercive field with increasing temperature indicates that the ferroelectric domains of the sample are easier to switch with temperature. The physical properties of ceramics like grain size, density and phase homogeneity are correlated to  $E_c$ ,  $P_s$ ,  $P_r$  and the squareness of the hysteresis loops. Ideally, the squareness parameter is equal to 2. Since larger grain size improves the ferroelectric properties the squareness of  $P$ - $E$  loops also improve with the grain size. According to Haertling and Zimmer, the squareness of a  $P$ - $E$  loop is determined by the following relation-

$$R_{sq} = \frac{P_r}{P_s} + \frac{P_{1.1E_c}}{P_r} \quad (7)$$

Where,  $R_{sq}$  is the squareness of hysteresis loop,  $P_s$  is saturation polarization,  $P_r$  is remnant polarization and  $P_{1.1E_c}$  is the polarization at an electric field equal to 1.1 times the coercive field ( $E_c$ ). The calculated values of  $R_{sq}$  for BCZT sample is 1.516, 1.38, 1.498, 1.347, 1.163 respectively at 25°C, 50°C, 75°C, 100°C, 125°C of PE loops. For all the temperatures the respective  $R_{sq}$  values are approximately near 1.5 indicating a better homogeneity and uniformity in grain size of the sample.

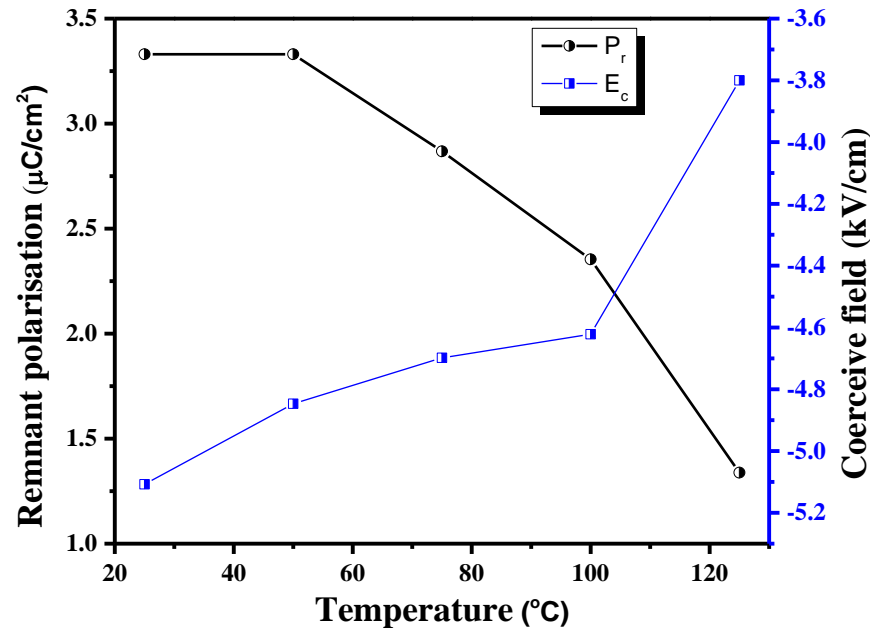


Fig. 8 Variation of remnant polarization ( $P_r$ ) and coercive field ( $E_c$ ) for BCZT ceramic at different temperatures and measured at 15kV/cm electric field

The hysteresis loops of BCZT ceramic plotted at different electric fields at 100°C (close to phase transition temperature) are shown in fig. 9. When the electric field is increased up to 20kV/cm the maximum polarization, the saturation polarization and the remnant polarization also found to increase. Since all the ferroelectric materials exhibit dipole reorientation and the domain growth, this type of typical behavior is quite expected. When the electric field intensity is less, the domain motion is driven slowly as the energy is not enough. When the intensity of electric field is slowly increased the overlapped domains start migrating and switching. Further on significantly increasing the electric field the domains are transformed and aligned directionally at 180° to the existence of domain wall resistance. Further, increasing the electric field leads to the domain reorientation in the path of the applied field. And finally, the conventionally saturated hysteresis loops are formed.

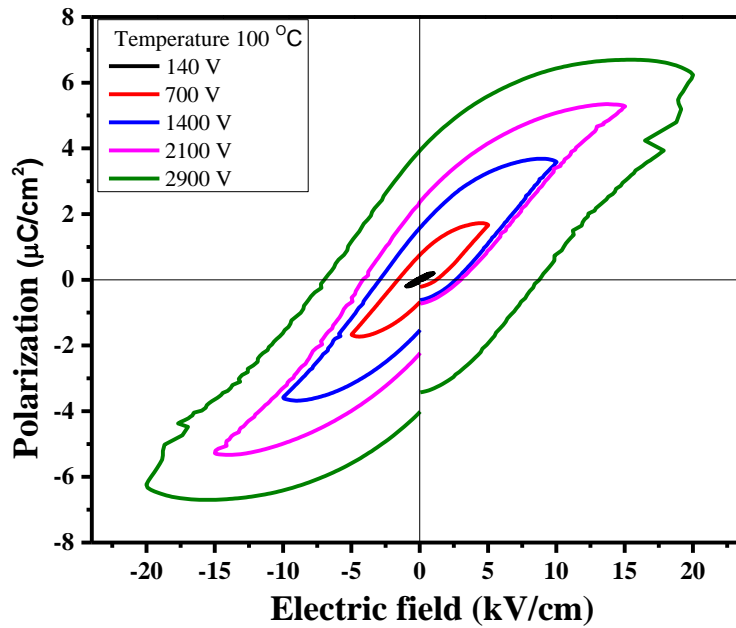


Fig. 9 P-E loops of BCZT ceramics at different voltages

In order to measure the energy storage performances, the charge storage density ( $Q_c$ ), the recoverable energy density ( $W_{rec}$ ), loss energy density ( $W_{loss}$ ), the total energy density ( $W_{total}$ ) and the energy storage efficiency ( $\eta$ ) of the ceramic are determined with the help of P-E loops. Here  $W_{rec}$  is equal to the area enclosed by the discharge polarization curve and the y-axis and  $W_{loss}$  is the energy density loss due to domain reorientation and leakage conduction, shown by the enclosed area of the charge and discharge polarization curve. The fig. 10 gives an idea about the  $W_{rec}$  (shown in yellow) and the  $W_{loss}$  (the green area). The energy storage efficiency is estimated using the following relations: -

$$W_{total} = \int_0^{P_{max}} E dP = W_{rec} + W_{loss} \quad (8)$$

$$W_{rec} = \int_{P_r}^{P_{max}} E dP \quad (9)$$

$$\eta\% = \frac{W_{rec}}{W_{total}} \times 100 \quad (10)$$

For better energy storage performances reduced remnant polarization and large maximal polarization are required so that the recoverable energy density and energy storage efficiency are improved [37]. The larger energy storage efficiency is an indicative of small loss in the form of hysteresis. The energy storage density ( $Q_c = P_s - P_r$ ), of a ferroelectric capacitor is measured from P-E loop at zero electric field. It is also expected that  $Q_c$  will increase with increasing electric field from zero to maximum. The increasing values of  $Q_c$  with electric field for 100 °C (close to  $T_c$ ) are presented in Table 2. The energy storage efficiency of the BCZT ceramic at various temperatures is tabulated in Table 3. It is seen that the energy storage efficiency ( $\eta$ ) increases with temperature because of the reduction of energy loss as shown in Fig. 11. The minimum energy storage efficiency is 24.7% at 25°C (room temperature) and the maximum is 44.3% at 125°C.

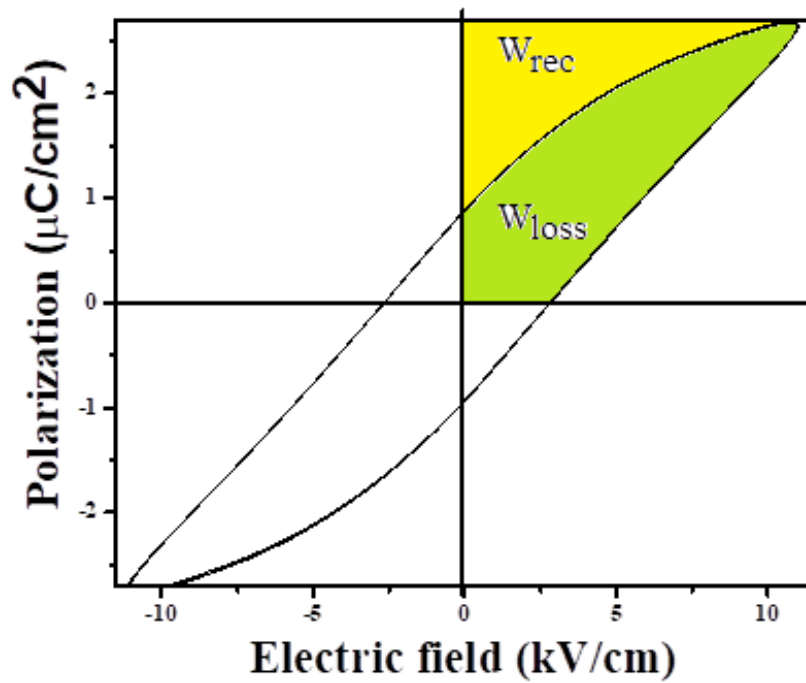


Fig. 10 Schematic diagram for calculation of energy storage efficiency from P-E loop

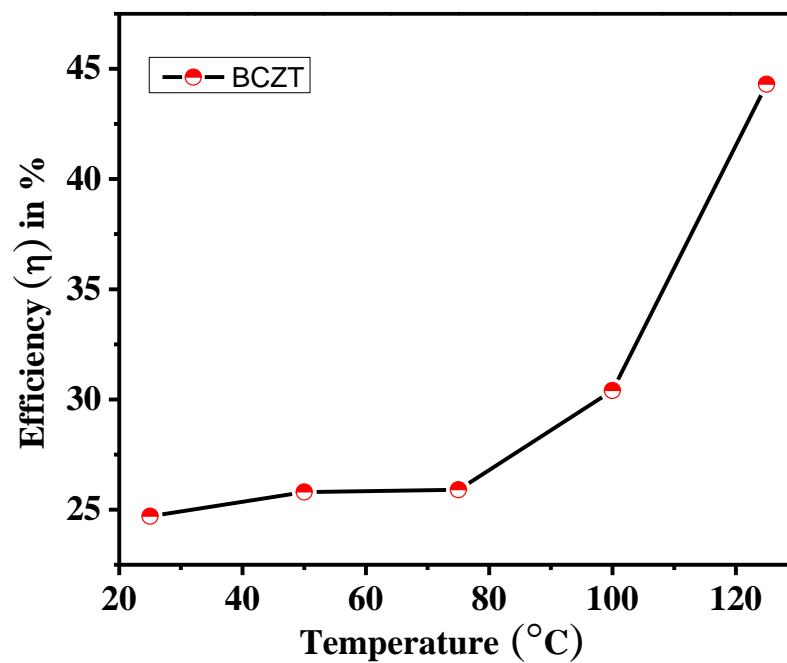


Fig. 11 Variation of energy storage efficiency ( $\eta$ ) with temperature of BCZT ceramic measured

#### 4. CONCLUSIONS

The present article reports the dielectric and energy storage performance of BCZT ceramic prepared using the solid-state reaction method calcined at 1300 °C for 5 h. From the results of XRD and Raman spectroscopy, it is evident that BCZT is polycrystalline and of perovskite crystal structure with tetragonal phase. SEM micrograph has shown that average grain size of the ceramic is 3.3  $\mu\text{m}$  which is considerably good to obtain the excellent ferroelectricity and dielectric properties. In the temperature-dependent dielectric studies, the dielectric anomaly pertaining to the phase transition was observed. The tetragonal to cubic phase transition is observed at 83°C. Modified Curie–Weiss law suggests that value of diffusivity is 1.7 which is approaching towards relaxor ferroelectrics. The results showed that dielectric permittivity and dielectric loss change little in the studied frequency range. The energy storage properties of lead-free BCZT ceramic are studied as a function of temperature. The highest energy storage efficiency is 44.3% for which the total energy density is 35.9 J/cm<sup>3</sup> at 125°C. The BCZT ceramic is a promising lead-free material for energy storage capacitor application.

Caption to the figures

Fig. 1 X-ray diffraction patterns of BCZT ceramic calcined at 1300 °C

Fig. 2(a) SEM micrograph of BCZT ceramic pellet sintered at 1350°C (b) grain size distribution of BCZT pellet

Fig. 3 Raman spectra of BCZT ceramic at room temperature

Fig. 4(a) Dielectric constant and (b) dielectric loss of BCZT ceramic as a function of temperature at 500kHz and 1MHz

Fig. 5 Dielectric constant of BCZT ceramic as a function of frequency at different temperatures

Fig. 6 Dielectric permittivity data fitted to the modified Curie–Weiss law for BCZT ceramic at 500 kHz

Fig. 7 P–E loops of BCZT ceramics at different temperatures sintered at 1350°C

Fig. 8 Variation of remnant polarization ( $P_r$ ) and coercive field ( $E_c$ ) for BCZT ceramic at different temperatures and measured at 15kV/cm electric field

Fig. 9 P–E loops of BCZT ceramics at different voltages

Fig. 10 Schematic diagram for calculation of energy storage efficiency from P-E loop

Fig. 11 Variation of energy storage efficiency ( $\eta$ ) with temperature of BCZT ceramic measured at 15kV/cm

#### REFERENCES

- [1] Y Xu, 2013 In Ferroelectric materials and their applications. Elsevier.
- [2] L W Martin, A M Rappe, Thin-film ferroelectric materials and their applications. *Nature Reviews Materials*, 2(2), 1-14 (2016)
- [3] P Kour, P Kumar, S K Sinha, M. Kar, Electrical properties of calcium modified PZT (52/48) ceramics. *Solid state communications*, **190**, 33-39 (2014)
- [4] S Rout, L Biswal, K Moharana, L Priyadarshini, A K Parida, R N P Choudhary, B Behera, Comprehensive analysis of structural, optical, dielectric and electrical properties of novel compound ( $\text{K}_{0.5}\text{Bi}_{0.5}\text{CaTi}_2\text{O}_6$ ) for multifaceted applications. *Journal of Alloys and Compounds*, **1013**, 178596 (2025)
- [5] N Kumar, R Kurchania, R J Ball, C R Bowen, S K Mittal, K L Yadav, J Rani, Enhanced dielectric, ferroelectric and piezoelectric properties of lead-free (Ba, Ca)(Sn, Ti)O<sub>3</sub> ceramics by optimisation of sintering temperature. *J. All. Compds.* **989** 174358 (2024)
- [6] O M Hemeda, B I Salem, H Abdelfatah, G Abdelsatar, M Shihab, Dielectric and ferroelectric properties of barium zirconate titanate ceramics prepared by ceramic method. *Phys. B: Cond. Matt.*, **574**, 411680 (2019)
- [7] N Binhayeeniyi, P Sukvisut, C Thanachayanont, S Muensit, Physical and electromechanical properties of barium zirconium titanate synthesized at low-sintering temperature. *Mater. Lett.* **64**(3), 305-308 (2010)
- [8] J Peng, D Shan, Y Liu, K Pan, C Lei, N He, Q Yang, A thermodynamic potential for barium zirconate titanate solid solutions. *npj Comp. Mater.* **4**, 66 (2018)
- [9] M Acosta, N Novak, G A Rossetti, J Rödel, Mechanisms of electromechanical response in  $(1-x)\text{Ba}(\text{Zr}_{0.2}\text{Ti}_{0.8})\text{O}_3-x(\text{Ba}_{0.7}\text{Ca}_{0.3})\text{TiO}_3$  ceramics. *Appl. Phys. Lett.* 107(14), (2015)
- [10] P Kantha, K Pengpat, P Jarupoom, U Intatha, G Rujijanagul, T Tunkasiri, Phase formation and electrical properties of BNLt–BZT lead-free piezoelectric ceramic system. *Curr. Appl. Phys.* **9**(2), 460-466 (2009)

- [11] P Elorika, S Anwar, Local heterogeneities and order-disorder: An approach to tailor BaTi<sub>1-x</sub>Zr<sub>x</sub>O<sub>3</sub> ceramics properties. *J. Mol. Struct.* **1299** 137158 (2024)
- [12] B K Pandey, A Kumar, K P Chandra, A R Kulkarni, S K Jayaswal, K Prasad, Electrical properties of 0.5(Ba<sub>0.7</sub>Ca<sub>0.3</sub>)TiO<sub>3</sub>–0.5Ba(Zr<sub>0.2</sub>Ti<sub>0.8</sub>)O<sub>3</sub>/PVDF nanocomposites. *J. Adv. Dielec.* **8(04)**, 1850027 (2018)
- [13] F Cordero, F Craciun, M Dinescu, N Scarisoreanu, C Galassi, W Schranz, V Soprunyuk, Elastic response of (1– x)Ba(Ti<sub>0.8</sub>Zr<sub>0.2</sub>)O<sub>3</sub>–x(Ba<sub>0.7</sub>Ca<sub>0.3</sub>)TiO<sub>3</sub> (x= 0.45–0.55) and the role of the intermediate orthorhombic phase in enhancing the piezoelectric coupling. *Appl. Phys. Lett.* **105(23)**, (2014)
- [14] L Zhang, M Zhang, L Wang, C Zhou, Z Zhang, Y Yao, X Ren, Phase transitions and the piezoelectricity around morphotropic phase boundary in Ba(Zr<sub>0.2</sub>Ti<sub>0.8</sub>)O<sub>3</sub>–x(Ba<sub>0.7</sub>Ca<sub>0.3</sub>)TiO<sub>3</sub> lead-free solid solution. *Appl. Phys. Lett.* **105(16)** (2014)
- [15] K S Srikanth, M K Hooda, H Singh, V P Singh, R Vaish, Structural and photocatalytic performance of (Ba, Ca)TiO<sub>3</sub>–Ba(Sn, Ti)O<sub>3</sub> ferroelectric ceramics. *Mater. Sci. Semi. Process.* **79** 153-160 (2018)
- [16] A Mehta, P Kumar, P Kumar, P Sharma, C Prakash, Synthesis, dielectric and ferroelectric properties in BSCT ceramics. *Curr. Appl. Phys.* **68**, 12-19 (2024)
- [17] P K Panda, B Sahoo, V Suresh Kumar, E D Politova, Effect of Zr<sup>4+</sup> on piezoelectric, dielectric and ferroelectric properties of barium calcium titanate lead-free ceramics. *J. Adv. Dielec.* **11** 2150024 (2021)
- [18] J P Praveen, K Kumar, A R James, T Karthik, S Asthana, D Das, Large piezoelectric strain observed in sol–gel derived BZT–BCT ceramics. *Curr. Appl. Phys.* **14(3)**, 396-402 (2014)
- [19] S P Kharat, S K Gaikwad, P G Nalam, R C Kambale, A R James, Y D Kolekar, C V Ramana, Effect of Crystal Structure and Phase on the Dielectric, Ferroelectric, and Piezoelectric Properties of Ca<sup>2+</sup>-and Zr<sup>4+</sup>-Substituted Barium Titanate Cryst. Growth. & Design. **22(9)**, 5571-5581 (2022)
- [20] P Sharma, P Kumar, R S Kundu, J K Juneja, N Ahlawat, R Punia, Structural and dielectric properties of substituted barium titanate ceramics for capacitor applications. *Ceram. Inter.* **41(10)**, 13425-13432 (2015)
- [21] X Yan, K H Lam, X Li, R Chen, W Ren, X Ren, K K Shung, Correspondence: Lead-free intravascular ultrasound transducer using BZT–50BCT ceramics. *IEEE trans. Ultrason. Ferroelectr. Freq. control* **60(6)** 1272-1276 (2013)
- [22] N Cucciniello, A R Mazza, P Roy, S Kunwar, D Zhang, H Y Feng, Q Jia, Anisotropic properties of epitaxial ferroelectric lead-free 0.5[Ba(Ti<sub>0.8</sub>Zr<sub>0.2</sub>)O<sub>3</sub>]-0.5(Ba<sub>0.7</sub>Ca<sub>0.3</sub>)TiO<sub>3</sub> films. *Mater.* **16(20)**, 6671 (2023)
- [23] Z Wang, Z Cai, H Wang, Z Cheng, J Chen, X Guo, H Kimura, Lead-free 0.5Ba (Ti<sub>0.8</sub>Zr<sub>0.2</sub>)O<sub>3</sub>-0.5(Ba<sub>0.7</sub>Ca<sub>0.3</sub>)TiO<sub>3</sub> thin films with enhanced electric properties fabricated from optimized sol-gel systems. *Mater. Chem. Phys.* **186**, 528-533 (2017)
- [24] H L Sun, Q J Zheng, Y Wan, Y Chen, X Wu, K W Kwok, H L W Chan, D M Lin, Correlation of grain size, phase transition and piezoelectric properties in Ba<sub>0.85</sub>Ca<sub>0.15</sub>Ti<sub>0.90</sub>Zr<sub>0.10</sub>O<sub>3</sub> ceramics. *J. Mater. Sci. Mater. Elect.* **26**, 5270-5278 (2015)
- [25] K Orlik, Y Lorgouilloux, P Marchet, A Thuault, F Jean, M Rguiti, C Courtois, Influence of microwave sintering on electrical properties of BCTZ lead free piezoelectric ceramics. *J. Eur. Ceram. Soc.* **40(4)**, 1212-1216 (2020)
- [26] W Li, X Ren, Large piezoelectric effect in Pb-free ceramics. *Phys. Rev. Lett.* **103(25)**, 257602 (2009)
- [27] S Sasikumar, R Saravanan, S Saravana Kumar, Investigation on charge density, piezoelectric and ferroelectric properties of (1– x)Ba(Zr<sub>0.2</sub>Ti<sub>0.8</sub>)O<sub>3</sub>–x(Ba<sub>0.7</sub>Ca<sub>0.3</sub>)TiO<sub>3</sub> lead-free piezoceramics. *J. Mater. Sci.: Mater. Electron.* **29**, 1198-1208 (2018)
- [28] P Wang, Y Li, Y Lu, Enhanced piezoelectric properties of (Ba<sub>0.85</sub>Ca<sub>0.15</sub>)(Ti<sub>0.9</sub>Zr<sub>0.1</sub>)O<sub>3</sub> lead-free ceramics by optimizing calcination and sintering temperature. *J. Eur. Ceram. Soc.* **31(11)**, 2005-2012 (2011)
- [29] M Sutapun, W Vittayakorn, R Muanghlua, N Vittayakorn, High piezoelectric response in the new coexistent phase boundary of 0.87BaTiO<sub>3</sub>–(0.13–x)BaZrO<sub>3</sub>–xCaTiO<sub>3</sub>. *Mater. Design.* **86** 564-574 (2015)
- [30] H J Sumona, A Al Mahmood, M B Islam, J H Kasem, M S Rahman, Modification of structural, morphological, and dielectric properties of barium calcium titanate ceramics with yttrium addition. *Heliyon* **10(5)**, (2024)
- [31] J G Maier, M Kuhfuß, D Urushihara, A Gadelmawla, N H Khansur, D Hall, M Algueró, A Martin, K I Kakimoto, K G Webber, Influence of grain size on electromechanical properties of (Ba, Ca)(Zr, Ti)O<sub>3</sub>: A multiscale analysis using spark plasma sintering and aerosol deposition. *Ceram. Inter.* **50(15)**, 26780-26791 (2024)
- [32] I V Lisnevskaya, I A Aleksandrova, A N Savinov, Lead-Free Multiferroic Barium-Calcium Zirconate-Titanate & Doped Nickel Ferrite Composites. *J. Compos. Sci.* **7(1)**, 2 (2022)
- [33] T Mitsui, W B Westphal, Dielectric and X-Ray Studies of Ca<sub>x</sub>Ba<sub>1-x</sub>TiO<sub>3</sub> and Ca<sub>x</sub>Sr<sub>1-x</sub>TiO<sub>3</sub>. *Phys. Rev.* **124(5)**, 1354 (1961)
- [34] T Zaman, M K Islam, M A Rahman, A Hussain, M A Matin, M S Rahman, Mono and co-substitution of Sr<sup>2+</sup> and Ca<sup>2+</sup> on the structural, electrical and optical properties of barium titanate ceramics. *Ceram. Inter.* **45(8)**, 10154-10162 (2019)
- [35] M H Khedhri, N Abdelmoula, H Khemakhem, R Douali, F Dubois, Structural, spectroscopic and dielectric properties of Ca-doped BaTiO<sub>3</sub>. *Appl. Phys. A.* **125**, 1-13 (2019)
- [36] P Kumar, S Singh, J K Juneja, C Prakash, K K Raina, Influence of calcium substitution on structural and electrical properties of substituted barium titanate. *Ceram. Inter.* **37(5)**, 1697-1700 (2011)
- [37] D Roy, S B Krupanidhi, Pulsed excimer laser ablated barium titanate thin films. *Appl. Phys. Lett.* **61(17)**, 2057-2059 (1992)

#### AUTHORS CONTRIBUTIONS

All authors contributed to the study conception and design. Material preparation, data collection and analysis were performed by Pawan Kumar, G Nag Bhargavi and Anjali Oudhia. The first draft of the manuscript was written by G Nag Bhargavi. Tanmaya Badapanda has conceptualized and designed the manuscript and revised it critically for important intellectual content. Dr. Sanjib Kumar Rout has provided the instrumentation facility for collecting data. All authors read and approved the final manuscript.”